*Review*

# Nanoplatforms Potentiated Ablation-Immune Synergistic Therapy through Improving Local Control and Suppressing Recurrent Metastasis

Zixuan Wei [1,2,†], Xiaoya Yu [1,†], Mao Huang [2], Liewei Wen [2,*] and Cuixia Lu [1,*]

1   Medical College, Guangxi University, Nanning 530004, China; qiangkunxuan@163.com (Z.W.); yuxiaoya0108@163.com (X.Y.)
2   Guangdong Provincial Key Laboratory of Tumor Interventional Diagnosis and Treatment, Zhuhai People's Hospital (Zhuhai Hospital Affiliated with Jinan University), Jinan University, Zhuhai 519000, China; huangm43@mail2.sysu.edu.cn
*   Correspondence: wenliewei@ext.jnu.edu.cn or wenner1989@163.com (L.W.); lucuixia@gxu.edu.cn (C.L.)
†   These authors contributed equally to this work.

**Abstract:** Minimally invasive ablation has been widely applied for treatment of various solid tumors, including hepatocellular carcinoma, renal cell carcinoma, breast carcinomas, etc. In addition to removing the primary tumor lesion, ablative techniques are also capable of improving the anti-tumor immune response by inducing immunogenic tumor cell death and modulating the tumor immune microenvironment, which may be of great benefit to inhibit the recurrent metastasis of residual tumor. However, the short-acting activated anti-tumor immunity of post-ablation will rapidly reverse into an immunosuppressive state, and the recurrent metastasis owing to incomplete ablation is closely associated with a dismal prognosis for the patients. In recent years, numerous nanoplatforms have been developed to improve the local ablative effect through enhancing the targeting delivery and combining it with chemotherapy. Particularly, amplifying the anti-tumor immune stimulus signal, modulating the immunosuppressive microenvironment, and improving the anti-tumor immune response with the versatile nanoplatforms have heralded great application prospects for improving the local control and preventing tumor recurrence and distant metastasis. This review discusses recent advances in nanoplatform-potentiated ablation-immune synergistic tumor therapy, focusing on common ablation techniques including radiofrequency, microwave, laser, and high-intensity focused ultrasound ablation, cryoablation, and magnetic hyperthermia ablation, etc. We discuss the advantages and challenges of the corresponding therapies and propose possible directions for future research, which is expected to provide references for improving the traditional ablation efficacy.

**Keywords:** tumor ablation; immunotherapy; nanoparticles; synergistic anti-tumor effect

## 1. Introduction

Tumor ablation is an imaging-guided, minimally invasive surgical procedure that is commonly used to treat solid tumors such as liver, kidney, lung, and brain tumors. During such a procedure, a needle-like probe guided by ultrasound, CT, or MRI is inserted into a solid tumor. Chemotherapy, alcohol, microwaves, radio waves, laser, or a freezing agent are delivered through this probe to kill the tumor cells [1,2,2–4]. The imaging-guided procedure was initially performed for diagnosis by needle biopsy but exploited for direct therapeutic intervention shortly after. In 1983, Sugiura and colleagues described the direct injection of absolute ethanol into small hepatocellular carcinoma (HCC) under ultrasound guidance [5], and this work was soon followed by the direct injection of chemotherapy into solid tumors of the liver, pancreas, pelvis, and lung [6–11]. In 1993, Rossi and co-workers first used radiofrequency ablation (RFA) to treat small HCC [12]. Microwave ablation (MWA) was first performed by Seki et al. in 1994 to treat HCC of less than 2 cm [13]. Cryoprobes were

used to treat lesions as early as the 1960s [14–16], and the technology development over recent decades has expanded their clinical applications in oncotherapy, including treatment of prostate cancer [17–22]. Compared with chemotherapy, radiotherapy, and conventional surgery, tumor ablation has the advantages of being less invasive, more effective and safer, more cost-efficient, and having a larger indication range [23–27]. Currently, tumor ablation is included in the guidelines for the treatment of a variety of solid tumors (Scheme 1). RFA, MWA, cryoablation, and anhydrous alcohol have been recommended as local treatment for liver cancer [28–30]. Ablation has also become a well-established local therapy for metastatic or recurrent tumors to achieve NED (tumor-free state) or relieve symptoms and cancerous bone pain [31–34]. Although ablation therapy is an effective method for the local destruction of tumor masses, it remains a palliative measure in the treatment of advanced and disseminated tumors [35]. However, it is becoming increasingly evident that this limitation can be rectified by the use of intra-tumor immunostimulants to enhance the potential anti-tumor immune response induced by ablation therapy [36–38]. Unlike surgical resection of the tumor, ablation interventions result in in situ coagulative tumor necrosis with the release of tumor antigens and danger-signaling molecules, which in turn may potentially activate or enhance the body's anti-tumor immune response.
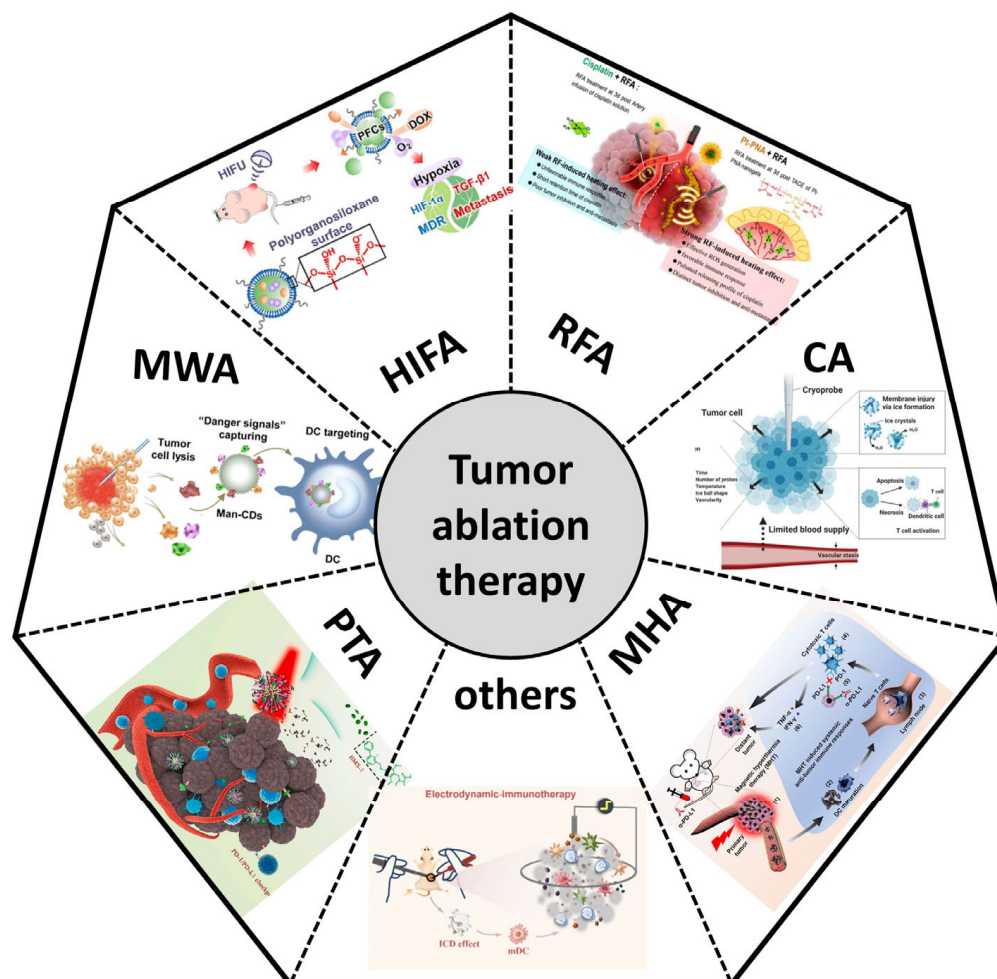


**Scheme 1.** Overview of tumor ablation therapy sensitized by nanoplatforms.

However, tumors have developed mechanisms to create an immunoreactive tumor microenvironment (TME); thus, the anti-tumor immune response stimulated by ablation alone is generally modest. There is increasing evidence according to which the localized delivery of immunomodulators can boost ablation-induced anti-tumor immunity [39]. Accordingly, tumor ablation in combination with localized immunotherapy has increasingly been used

to treat various benign and malignant tumors in preclinical and clinical research [29,40]. Nanoplatforms are macromolecular materials composed of nanoparticles such as nanotubes, nanosheets, and mesoporous materials. They can be used as drug carriers for treating cancers [41–44]. Multifunctional nanoplatforms can deliver multiple drugs with optimized drug encapsulation and therapeutic efficiency. In the context of cancer treatment, nanoparticle-based drug delivery systems have shown great potential in improving treatment efficacy and reducing toxicity. Furthermore, the ability of nanoparticles to enhance drug accumulation in tumor tissues and the immune system makes them an attractive platform for enhancing ablation-immune synergistic therapy. Other than serving as drug carriers, nanoplatforms themselves have radiotherapy potentiation capability, photothermal and photodynamic effects, magnetic hyperthermia effects, and immunomodulatory properties [45,46]. Nanoparticles can modulate the immunosuppressive TME to induce and enhance immune responses. They can also be used as adjuvants for cancer vaccines to boost vaccine-induced anti-tumor immune responses. Recent research demonstrates the efficacy of immunomodulatory biomaterials in preclinical models of cancer and autoimmune diseases and discusses the potential of these materials for use in combination with other immunotherapeutic approaches [47]. Furthermore, nanoplatforms can be used in imaging techniques to identify and locate tumors, guide ablation procedures, and monitor drug response (Table 1). These characteristics make nanoplatforms an ideal material for integrating chemotherapy, immunotherapy, and ablation therapy to achieve synergistic anti-cancer outcomes.

**Table 1.** Nanoplatforms potentiated ablation-immune synergistic therapy.

| Ablation Technique | Nanoplatforms | Immune Activating Strategies | Immunity Effect | Experimental Models | Type of Cancer | Ref. |
|---|---|---|---|---|---|---|
| Radiofrequency Ablation (RFA) | hemin and LOX co-loaded CaCO3-encapsulated PLGA nanoreactors (HLCaP NRs) | PD-1 blockade immune checkpoint blockade | Primed antitumor immunity to effectively suppress the growth of both residual and metastatic tumors, | 4T1 tumors on mice, H22 tumors on Balb/c mice, VX2 tumors on New Zealand rabbits | Breast cancer, liver cancer | [48] |
| RFA | Poly (N-iso prylacrylamide-b-methyl acrylic acid) nanogels (Pt-PNA) | Inducing a favorable immune response | inducing a favorable immune response and enhancing the synergistic antitumor effect of RFA. | VX2 liver tumor in rabbits, | Liver cancer | [49] |
| High-Intensity Focused Ultrasound (HIFU) | Perfluorooctyl bromide (PFOB) nanoemulsions holding MnO$_2$ nanoparticles (MBP) | Triggered immunogenic cell death (ICD) | Elicited maturation of dendritic cells (DCs) facilitated activation of CD8$^+$ T cells, CD4$^+$ T cells, and NK cells. | 4T1 tumors on nude mice | Breast cancer | [50] |
| HIFU | PLGA-R837 particles and PLGA-MPLA particles | Adjuvants and immune checkpoint blockade | Stimulated immature DCs and naive T cells at tumor sites | CT26 tumors on Balb/c mice | Colon cancer | [51] |
| Microwave Ablation (MWA) | mannose-derived Carbon dots (Man-CDs) | Immune adjuvants | Promoted DCs maturation and secret cytokines such as IL-1β, IL-6 and TNF-α. | Hepa1–6 tumors on C57BL/6 mice | Liver cancer | [52] |

**Table 1.** *Cont.*

| Ablation Technique | Nanoplatforms | Immune Activating Strategies | Immunity Effect | Experimental Models | Type of Cancer | Ref. |
|---|---|---|---|---|---|---|
| MWA | aPDL1&IPI549@Gel | PD-1 blockade | Inhibited progression of residual tumors after inadequate ablation | CT26 tumors on Balb/c mice | Colon cancer | [53] |
| Magnetic Hyperthermia Ablation (MHA) | $CoFe_2O_4@MnFe_2O_4$ | PD-1 blockade | Promoted the maturation and activation of DCs and cytotoxic T cells | 4T1 tumors on Balb/c mice | Breast cancer | [54] |
| MHA | Ferrimagnetic vortex-domain iron oxide nanoring and graphene oxide (FVIOs-GO) | Triggered immunogenic cell death (ICD) | Promoted macrophage polarization to M1 phenotypes, and increases tumor-infiltrating T lymphocytes | 4T1 tumors on Balb/c mice | Breast cancer | [55] |
| Photothermal Ablation (PTA) | I-PEG2k-COOH capped Pt NPs(I-Pt NPs) | PD-L1 inhibitor (BMS-1) | Captured the antigen released from the ablated tumor cells, enhanced the antigen internalization | 4T1 tumors on Balb/c mice | Breast cancer | [56] |
| PTA | $Cu^{2+}$ and LOX into mPDA nanoparticles(mCuLP) | Triggered immunogenic cell death (ICD) | Promoted DC maturation and then T lymphocyte infiltration to kill tumor cells | 4T1 tumors on Balb/c mice | Breast cancer | [57] |
| PTA | CpG ODNs | CpG Toll-like receptor 9 (TLR9) agonist. | Induced maturation of DCs and activated immunogenic cell death (ICD) | B16F10 tumors on C57BL/6 mice | Melanoma | [58] |
| PTA | PLGA-ICG-R837 nanoparticles | R837 Toll-like receptor 7 (TLR7) agonist. | Activated immune system, inhibited growth of distant tumours. | 4T1 tumors on Balb/c mice, CT26 tumors on Balb/c mice | Breast cancer, Colorectal cancer | [59] |
| Electrodynamic therapy (EDT) | Pt–Pd@DON | Triggered immunogenic cell death (ICD) | Promoted the joint functions of ICD and $CD8^+$ T cell infiltration | 4T1 tumors on Balb/c mice | Breast cancer | [60] |

## 2. Classification and Characteristics of Tumor Ablation Therapy

In recent years, cancer treatment has seen tremendous progress with the development of novel therapeutic strategies such as ablation and immunotherapy. Ablation involves the physical destruction of cancer cells through methods such as heat, cold, or radiation, while immunotherapy aims to stimulate the patient's immune system to fight cancer. However, these approaches are not always effective on their own, and can have limitations such as toxicity and resistance (Table 2). To overcome these challenges, researchers have been exploring the use of nanoplatforms to deliver both ablation and immunotherapy agents simultaneously. This collaborative strategy has shown promising results in preclinical studies and holds great potential for the development of more effective cancer treatments.

**Table 2.** Different ablation applications using different techniques.

| Ablation Technique | Application | Advantages | Disadvantages |
|---|---|---|---|
| Radiofrequency Ablation (RFA) | Cancer treatment, arrhythmia treatment, pain management | Low risk, low cost, fast procedure, precise, minimal scarring, compatibility with pacemakers and metal implants | Limited penetration, can cause nerve damage, may require multiple sessions, not suitable for large tumors |
| High-Intensity Focused Ultrasound (HIFU) | Cancer treatment, uterine fibroid treatment | Non-invasive, precise, low risk of complications, no ionizing radiation, Large killing range | Limited penetration, requires image guidance, not suitable for all tumor types, expensive |
| Microwave Ablation (MWA) | Cancer treatment | Fast procedure, minimal scarring, can be performed on an outpatient basis, suitable for larger tumors, Ability to resist the influence of blood flow | Limited penetration, can cause nerve damage, may require multiple sessions, not suitable for all tumor types |
| Magnetic Hyperthermia Ablation (MHA) | Cancer treatment | Non-invasive, can target deep-seated tumors, can be combined with other therapies, low risk of complications | Requires magnetic nanoparticles to be delivered to the tumor site, currently in experimental stages |
| Cryoablation (CA) | Cancer treatment, pain management | Non-invasive, precise, low risk of complications, can be performed on an outpatient basis, low anesthesia requirements | Limited penetration, may require multiple sessions, not suitable for all tumor types, can cause nerve damage |
| Photothermal Ablation (PTA) | Cancer treatment | Non-invasive, precise, needle catheter ablation for hemostasis | Limited penetration, may require multiple sessions, not suitable for all tumor types, can cause skin damage |

*2.1. Radiofrequency Ablation*

During an RFA procedure, radiofrequency waves are sent through the probe into the surrounding tumor tissues, creating an alternating electric current that heats up and kills the tumor cells by coagulative necrosis. Each RFA treatment is about 30 min long, and the necrotic tissues are usually absorbed in situ. Compared with conventional tumor treatment methods, RFA is safer, less painful, and more cost-efficient. Additionally, patients usually have a fast recovery and can be discharged after 1–2 days of observation. However, RFA has limited effects on large tumors, and its anti-tumor efficacy is often affected by tumor heterogeneity [61,62]. For this reason, RFA is usually combined with other therapeutic modalities for integrative treatment of cancer [63]. For example, Li and colleagues created RFA-responsive cisplatin cross-linking poly(N-isoprylacrylamide-b-methyl acrylic acid) (PNA) nanogels (Pt-PNA) for triple therapies of ablation–chemo–embolization [49] (Figure 1A,B). Cisplatin is a popular metal ion-based antitumor drug that also exhibits RF-responsive thermal effects through the coordinate bonding between Pt (II) ions and carboxyl groups. The Pt-PNA nanogels can kill tumor cells through both the cytotoxic action of cisplatin and an RFA-induced thermal effect. In addition, the nanogels can rapidly spread to the tumor peripheral arteries and block the tumor blood supply elicited by temperature-sensitive sol–gel conversion to achieve transcatheter arterial chemoembolization (TACE) (Figure 1C–E). Yang and colleagues constructed unique pH-sensitive nanoreactors by co-encapsulating lipoxidase (LOX) and heme chloride with poly (lactic-co-glycolic acid) (PLGA) (HLCaP) using a $CaCO_3$-assisted double emulsion method. These nanoreactors

can utilize RFA-generated tumor debris as the fuel to continuously produce cytotoxic lipid radicals, inducing immunogenic cell death (ICD) and inhibiting the growth of residual tumors following RFA [48] (Figure 1F,G). Cao and colleagues found that radio frequency can potentially serve as a safe and effective physical adjuvant to boost vaccination [64]. In murine models of intradermal vaccination, RFA treatment of a small skin area ($2 \times 2$ cm$^2$) prior to intradermal delivery of ovalbumin or recombinant hemagglutinin can enhance vaccine-induced humoral and cellular immune responses with potency comparable to common chemical adjuvants. These adjuvant effects may be attributed to increased vaccine uptake and the maturation of dendritic cells (DCs) in the skin and draining lymph nodes (DLNs) following RFA (Figure 1H,I).
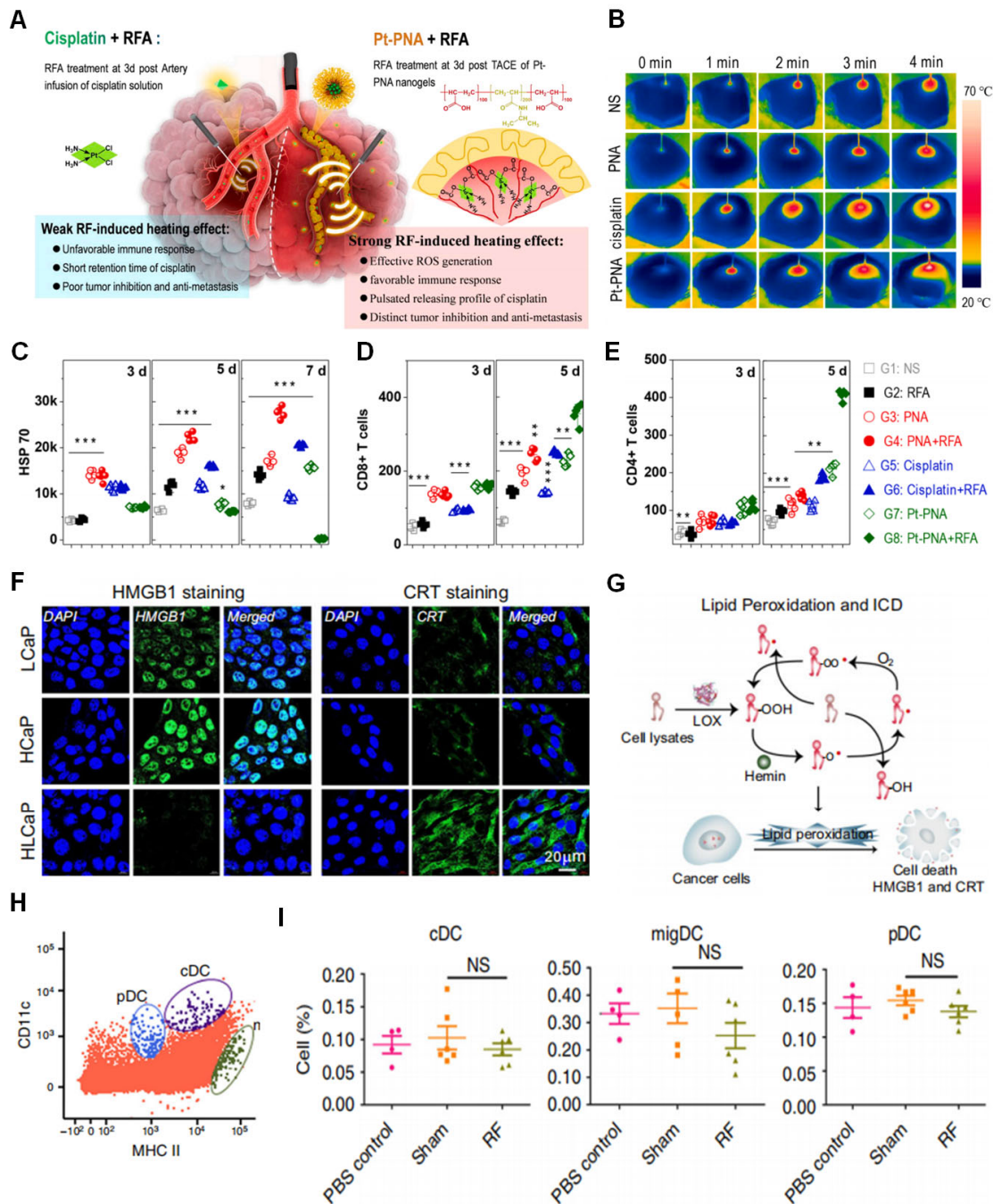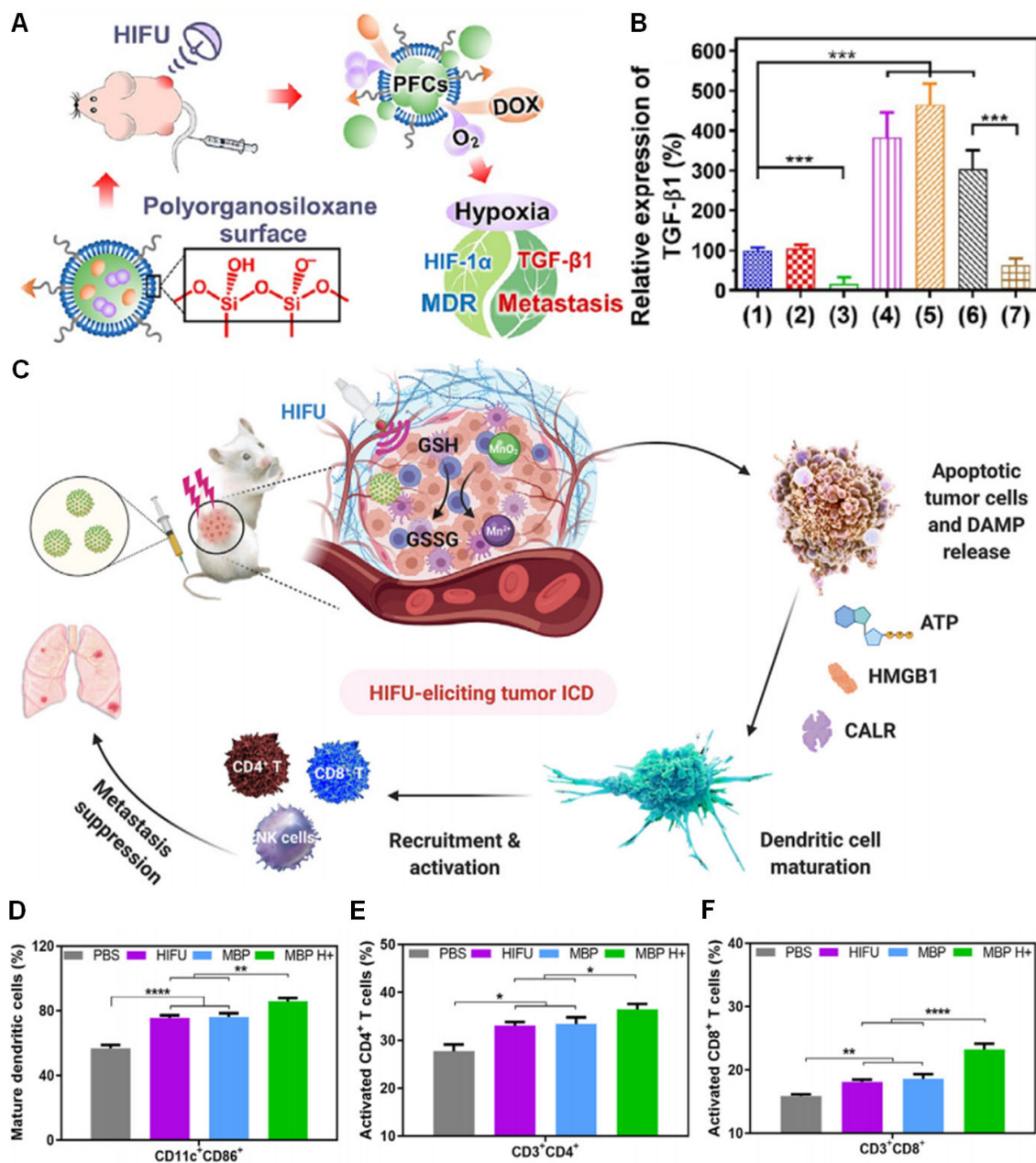


**Figure 1.** Example of nanomedicine-based RFA to activate immune responses. (**A**) Schematic illustration of double therapy with cisplatin and RFA and triple therapy (ablation–chemo–embolization)

with Pt-PNA nanogels and RFA. (**B**) Infrared thermal images of the liver treated with local injection of blank control (NS), PNA, cisplatin, or Pt-PNA in combination with RFA (100 W, up to 4.0 min). (**C**–**E**) HSP70 expression levels (**C**), infiltrating CD8$^+$ T cells (**D**), and infiltrating CD4$^+$ T-cells (**E**) in residual tumor tissues surrounding the tumor necrosis zone after treatment for a specific number of days (* $p < 0.05$; ** $p < 0.01$; *** $p < 0.001$). (**F**) 4T1 cells incubated with HCaP, LCaP, or HLCaP nanoreactors in the presence of cancer cell lysates were stained with HMGB1 and CRT antibodies, respectively. Confocal fluorescence images are shown. (**G**) Schematic illustration of HLCaP nanoreactor-mediated propagation of lipid peroxidation in the presence of cell lysates and subsequent induction of immunogenic cell death. (**H**,**I**) RF treatment increases antigen uptake and the maturation of DCs in dLNs in murine models of intradermal vaccination.

## 2.2. High-Intensity Focus Ultrasound

In ultrasound ablation (UA), also known as high-intensity focused ultrasound (HIFU), many ultrasound beams, guided by MRI or ultrasound, focus on the exact tumor area that requires treatment. The highly focused ultrasound energy heats up the targeted tumor tissues and causes coagulative necrosis of the tumor cells. The resulting tumor cell debris can activate the body's immune responses, inducing tumor ICD. The ability of HIFU to pass through overlying skin and tissues without damage has made it an attractive precision therapy for deep-seated tumors. However, the ultrasound energy decreases exponentially with the depth of the tissue, leading to insufficient intensity for certain deep-seated tumors. This problem can be remedied by introducing nanoparticles into tumor tissues to change the acoustic environment. Chen and colleagues designed and synthesized multifunctional organic–inorganic hybrid nano-vesicles of PLGA loaded with perfluorocarbon (PFC), the hydrophobic anti-tumor drug ruthenium complex (RuPOP), and superparamagnetic nano $Fe_3O_4$ [65]. The nano-vesicles were coated with an ultrathin silica shell to achieve double therapies of HIFU and HIFU-triggered explosive release of RuPOP. Hypoxia within the TME contributes to immune resistance of tumor cells [66] and limit the therapeutic efficacy of HIFU. To overcome this problem, Liang and colleagues constructed ultra-stable PFC nanodroplets (D-vPCs-O$_2$) to co-deliver oxygen and doxorubicin (DOX) to the target tumor [67]. The nanodroplets had an atomic polyorganosiloxane surface and pH-sensitive tumor-targeting peptide for tumor-specific cargo delivery (Figure 2A). HIFU was used to trigger the co-release of DOX and oxygen while enhancing ultrasound imaging, thereby enabling imaging-guided drug delivery. Mild-temperature HIFU (M-HIFU) not only triggered oxygen release, but also slightly increased tumor temperature and blood flow, further ameliorating tumor hypoxia. The chemotherapy and relief of hypoxia jointly downregulated the expression of transforming growth factor-β 1 (TGF-β1), thereby reducing the epithelial–mesenchymal transition (EMT) and inhibiting tumor metastasis (Figure 2B). When D-vPCs-O$_2$ was used with M-HIFU as a neoadjuvant, heat shock proteins were significantly downregulated, and tumor recurrence after high-temperature HIFU (H-HIFU) ablation was reduced. In clinical practice, HIFU as a stand-alone therapy cannot induce sufficient anti-tumor immune response to eradicate tumor metastasis or recurrence. Strategies to boost HIFU efficacy for inhibiting tumor metastasis and recurrence are under active development. Kuai and colleagues developed perfluorooctyl bromide (PFOB) nano-emulsions containing $MnO_2$ nanoparticles (MBPs) that can amplify HIFU-induced tumor ICD (Figure 2C) [50]. By simultaneously depleting the glutathione (GSH) and boosting HIFU-induced tumor ICD, MBPs can modulate the tumor immune microenvironment by inducing dendritic cell (DC) maturation and promoting CD8$^+$ and CD4$^+$ T cell activation, thereby inhibiting tumor growth and lung metastasis (Figure 2D–F).
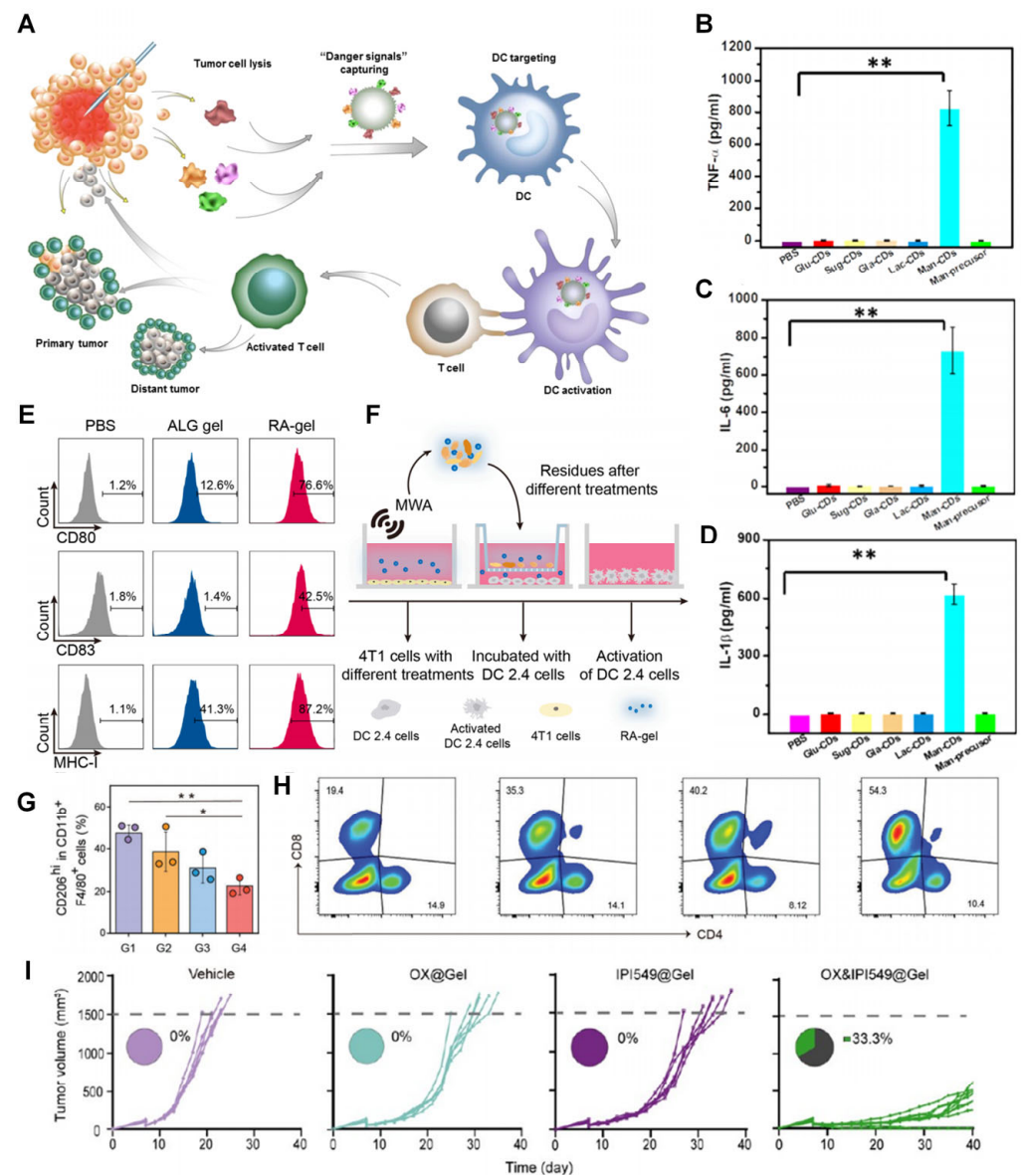
**Figure 2.** Example of nanomedicine-based HIFU to activate immune responses. (**A**) Schematic illustration of HIFU-triggered co-release of oxygen and DOX from PFC nanodroplets to alleviate hypoxia and inhibit tumor metastasis. (**B**) Relative expression levels of TGF-β1 of 4T1 cells after treatment. (1) PBS; (2) vPCs-$N_2$ + M-HIFU; (3) vPCs-$O_2$ + M-HIFU; (4) free DOX; (5) Doxil; (6) D-vPCs-$N_2$ + M-HIFU; (7) D-vPCs-$O_2$ + M-HIFU (n = 5, *** $p < 0.001$). (**C**) Schematic illustration of how MBPs enhance HIFU-induced tumor ICD. (**D**–**F**) The percentages of mature DCs (**D**), activated CD4$^+$ T cells (**E**), and activated CD8$^+$ T cells (**F**) in tumor tissues 72 h after treatment (* $p < 0.05$, ** $p < 0.01$, and **** $p < 0.0001$ compared with PBS or MBP H$^+$).

### 2.3. Microwave Ablation

Microwave ablation (MWA) uses heat generated from electromagnetic microwaves to induce the coagulative necrosis of tumor cells. MWA alone usually triggers a weaker immune response than RFA, possibly due to high temperature-induced tumor-associated antigen (TAA) inactivation. Nevertheless, compared with RFA, MWA has significant advantages because it can have deeper tissue penetration, better efficacy for larger tumors, and reduced sensitivity to the heat sink effect [68]. Hence, various strategies have been

developed to enhance the anti-tumor effects of MWA. Zhu's team proposes a $Ca^{2+}$-surplus alginate hydrogel plus MWA treatment to ablate tumors on both mice and rabbits, and to elicit antitumor immunity when synergized with $Mn^{2+}$. The metallo-alginate hydrogel acts as a microwave-susceptible and immunostimulatory biomaterial to reinforce the MWA therapy, which is promising for clinical translation [69]. Carbon dots (CDs) are carbon-based nanomaterials with fluorescence properties. Due to their excellent biocompatibility and abundant low-cost sources, CDs have found important applications in biomedicine [70]. Zhou and colleagues used mannose to synthesize CDs with a diameter of about 3 nm [52]. In in vitro experiments, these mannose-derived CDs effectively captured TAAs after MWA treatment and delivered them to DCs, promoting DC maturation and the secretion of cytokines such as IL-1β, IL-6, and TNF-α (Figure 3A–D). In mice, the intra-tumor injection of these CDs after MWA significantly inhibited liver metastasis and produced long-term immune memory to inhibit tumor recurrence. Hydrogels have excellent biological properties and are widely used as carriers for drug or cell delivery. Due to the fact that hydrogels can encapsulate TAAs or immunotherapeutic drugs for controlled release and promote the infiltration of immune cells, they can be used to enhance the efficacy of immunotherapy [71]. Due to the space confinement effect, the metal ions encapsulated in hydrogels can effectively boost MWA. Microwaves can rapidly heat up hydrogels without affecting the surrounding area; thus, the surrounding tissues are well protected during MWA. Cao and colleagues were the first to report an injectable, microwave-sensitive hydrogel with immunomodulatory properties, which boosted anti-tumor immunity elicited by combined MWA and immunotherapy [72]. The immunomodulatory hydrogel was prepared by introducing various immunostimulants and an immunoadjuvant (R837) into the alginate (ALG)-$Ca^{2+}$ hydrogel. The loaded R837 enhanced in situ vaccination with TAAs released after MWA and promoted DC maturation, eliciting potent anti-tumor immunity and suppressing distant metastasis in vivo (Figure 3E,F). Li and colleagues showed that the rapid tumor progression following inadequate MWA is mainly mediated by the so-called "cold" tumor immune environment, which is characterized by the enrichment of immunosuppressive factors and a lack of cytotoxic T lymphocytes infiltration [53]. In the same study, Li and colleagues designed and constructed a reactive oxygen species (ROS)-sensitive in situ hydrogel-based scaffold for the co-delivery of the selective PI3Kγ inhibitor IPI549 and an anti-programmed death ligand 1 antibody (aPDL1) for post-ablation cancer immunotherapy. IPI549 can reverse the immunosuppressive niche created by inadequate MWA and promote immune checkpoint blockade (ICB)-mediated anti-tumor immune response. The IPI549-loaded hydrogel can reshape the tumor immune microenvironment (TIME) by reducing the presence of $CD11b^+$ immunosuppressive cells (including myeloid-derived suppressor cells and tumor-associated macrophages (TAMs)) and enhancing the infiltration of $CD8^+$ T cells (Figure 3G,H). In combination with the continuous release of aPDL1, the ROS-responsive scaffold can trigger a strong anti-cancer immune response to create a "hot" tumor immune niche, degenerating/eradicating primary tumors, inhibiting the development of distant and diffuse metastases, and eliciting immunologic memory that provides long-lasting protection. Additionally, to combat the high invasiveness of residual tumor following inadequate MWA, Shen and colleagues developed a fibrin hydrogel scaffold for the co-delivery of IPI549 and the immunostimulatory chemotherapy Oxaliplatin (OX) for post-ablation cancer treatment [73]. In mouse CT26 colorectal cancer models, the IPI549 and OX-loaded hydrogel evoked robust systemic anti-tumor immunity to inhibit tumor growth and metastasis, and induced strong long-term immunologic memory against tumor recurrence (Figure 3I).
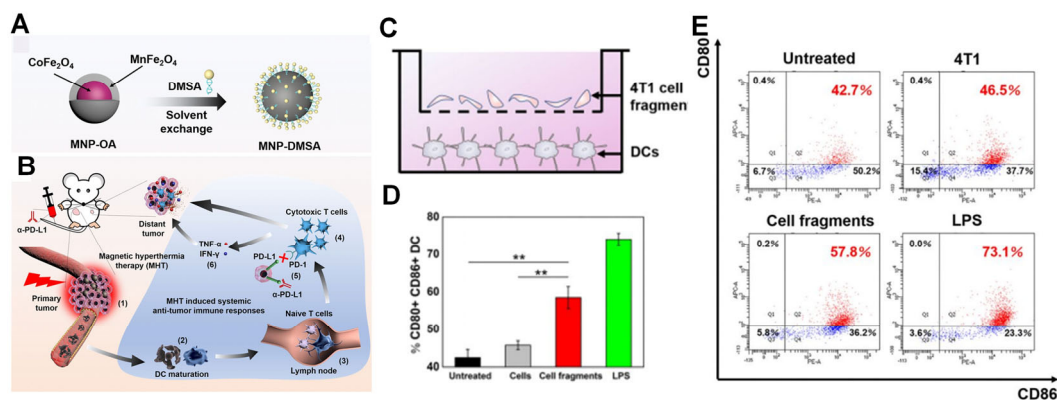
**Figure 3.** Example of nanomedicine-based MWA to activate immune responses. (**A**) Schematic illustration of how intra-tumoral mannose-derived CDs capture TAAs after MWA treatment and deliver them to DCs, promoting DC maturation and T cell activation, and inhibiting tumor growth and metastasis. (**B**–**D**) The concentrations of TNF-$\alpha$ (B), IL-6 (**C**), and IL-1$\beta$ (**D**) after specific treatment. (Student's *t* test was used, ** $p < 0.01$). (**E**) The expression levels of the surface markers CD80, CD83, and MHC-I in DC2.4 DCs after treatment with PBS, ALG gel, and R837-loaded ALG gel for 24 h. (**F**) Schematic illustration of a Transwell system for the evaluation of 4T1 residue-induced DC2.4 activation enhanced by R837-loaded ALG gel. (**G**,**H**) Quantification of TAMs-M2 (CD206hi) in CD11b$^+$F4/80$^+$ cell population (**G**) and flow cytometric analysis of CD8$^+$T cells (* $p < 0.05$, ** $p < 0.01$). (**H**) after specific treatment. G1, control gel; G2, aPDL1-loaded gel; G3, IPI549-loaded gel; G4, aPDL1 and IPI549-loaded gel. (**I**) Individual residual tumor growth curves after specific treatment. The pie chart represents the cure rate.

## 2.4. Magnetic Hyperthermia Ablation

Magnetic hyperthermia ablation (MHA) uses magnetic responsive materials to transform magnetic energy into thermal energy under the action of an alternating magnetic field to kill tumor cells. The mechanisms for thermal energy generation include eddy current loss, hysteresis loss, Néel relaxation, and Brownian relaxation. The magnetic field used in MHA has no tissue penetration limit, and does not produce any thermal effect on tissues in the

absence of magnetic responsive materials. Thus, MHA is a suitable therapy for deep-seated tumors, including large ones [74,75]. However, due to the difficulties in precisely targeting deep-seated tumors and achieving homogeneous heat distribution within the tumor, the clinical application of MHA is relatively rare [76,77]. PAN and colleagues synthesized monodisperse, high-performance superparamagnetic $CoFe_2O_4@MnFe_2O_4$ nanoparticles with a diameter of about 11.9 nm for MHA of primary tumors [54]. Using these nanoparticles, MHA can trigger the release of abundant TAAs to promote the maturation and activation of DCs and cytotoxic T cells, delivering effective immunotherapy for distant metastatic tumors in tumor-bearing mice (Figure 4).
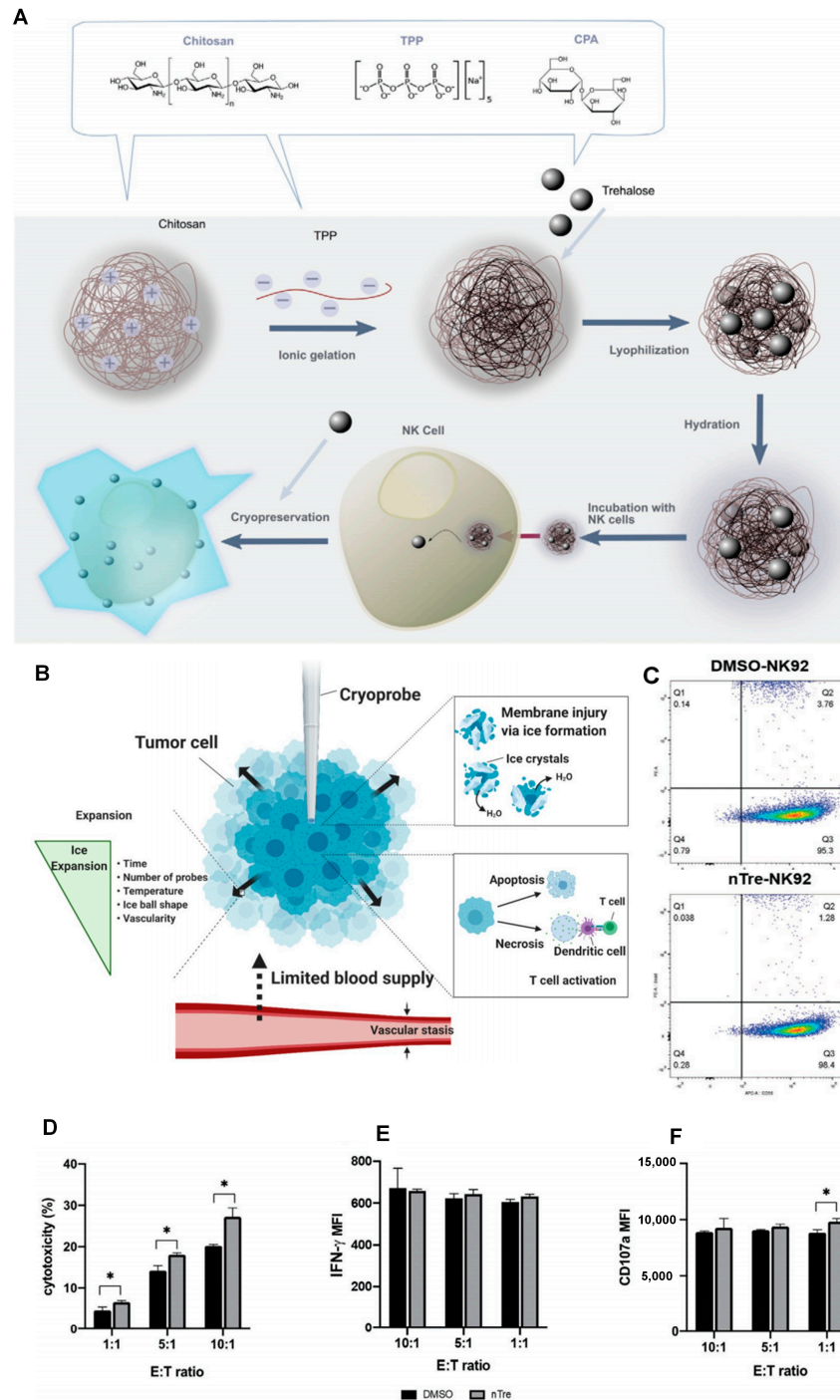


**Figure 4.** Example of nanomedicine-based MHA to activate immune responses. (**A**) Schematic illustration of the preparation of $CoFe_2O_4@MnFe_2O_4$ nanoparticles (MNP-OA) and DMSA-modified $CoFe_2O_4@MnFe_2O_4$ nanoparticles (MNP-DMSA). (**B**) Schematic illustration of how combined MHA and α-PD-L1 treatment activates anti-tumor immune responses to target metastatic tumors. (**C**) Schematic illustration of a Transwell system for the evaluation of DC maturation induced by MHA-generated 4T1 cell residues. (**D**,**E**) The percentage of matured DCs ($CD80^+$ $CD86^+$ DCs) (**D**) and representative FACS plots of CD80, CD86 expression on DCs gated by $CD11c^+$ cells (** $p < 0.01$).

## 2.5. Cryoablation

In cryoablation, a thin, hollow needle called a cryoprobe is placed directly into the target tumor. A freezing agent such as liquid nitrogen is pumped into the cryoprobe to freeze and kill the tumor cells by necrosis or apoptosis. Compared with RFA and MWA, cryoablation is less painful and has the benefit of a faster postoperative recovery [78]. Cryoablation is a relatively new option in oncotherapy and is most suitable for the treatment of elderly patients with tumors near the skin. Cryoablation also produces TAAs in situ that can activate the host's anti-tumor immunity and thus, it can serve as an adjuvant to enhance immunotherapy [79,80]. However, cryoablation has a few limitations. In clinical practice, cryoablation often fails to freeze and kill the entire target tumor due to the presence of a temperature gradient between the cryoprobe and the tumor tissue. In addition, surrounding healthy tissues may suffer cryogenic injury caused by off-target freezing [81]. Furthermore, cryoablation is suitable for treating small tumors but has little effect on large ones [82]. Hence, strategies to overcome these limitations are under active development to improve the clinical benefits of this convenient and cost-effective method. Increasing evidence has indicated that, by activating anti-tumor immune responses, cryoablation can work synergistically with drug-loaded nanoparticles to achieve desired therapeutic effects. Wang and colleagues developed a cold-responsive HCPN-CG nanoparticle composed of hyaluronic acid (HA), chitosan, PNIPAM-B and pluronic F127 (PF127) for cold-controlled co-delivery of chemotherapy (CPT) and a photothermal agent (ICG) to human breast tumors in situ [83]. When being cooled below 10 °C, this nanoparticle disassembles and releases the encapsulated agents to kill the tumor cells in co-ordination with cryoablation. Yao and colleagues prepared a simple and biocompatible chitosan-tripolyphosphate (CS-TPP) nanoparticle carrying trehalose, a cryoprotectant [84]. Trehalose can protect natural

killer (NK) cells near the target tumor from cryoinjury, preserving and enhancing the anti-tumor immunity following cryoablation (Figure 5). Notably, this method is capable of preserving surrounding healthy tissues as well. Chen and colleagues utilized PLGA to co-encapsulate an ICG and R837, a Toll-like receptor (TLR)-7 agonist, and an immune checkpoint inhibitor [59]. This nanoparticle can release R837 when stimulated by photothermal therapy, enhancing TAA-elicited anti-tumor immunity in mice. Notably, nanoparticles alone can change the mobility and penetrability of the tumor cell membrane, sensitizing the cells to cryoablation [85].
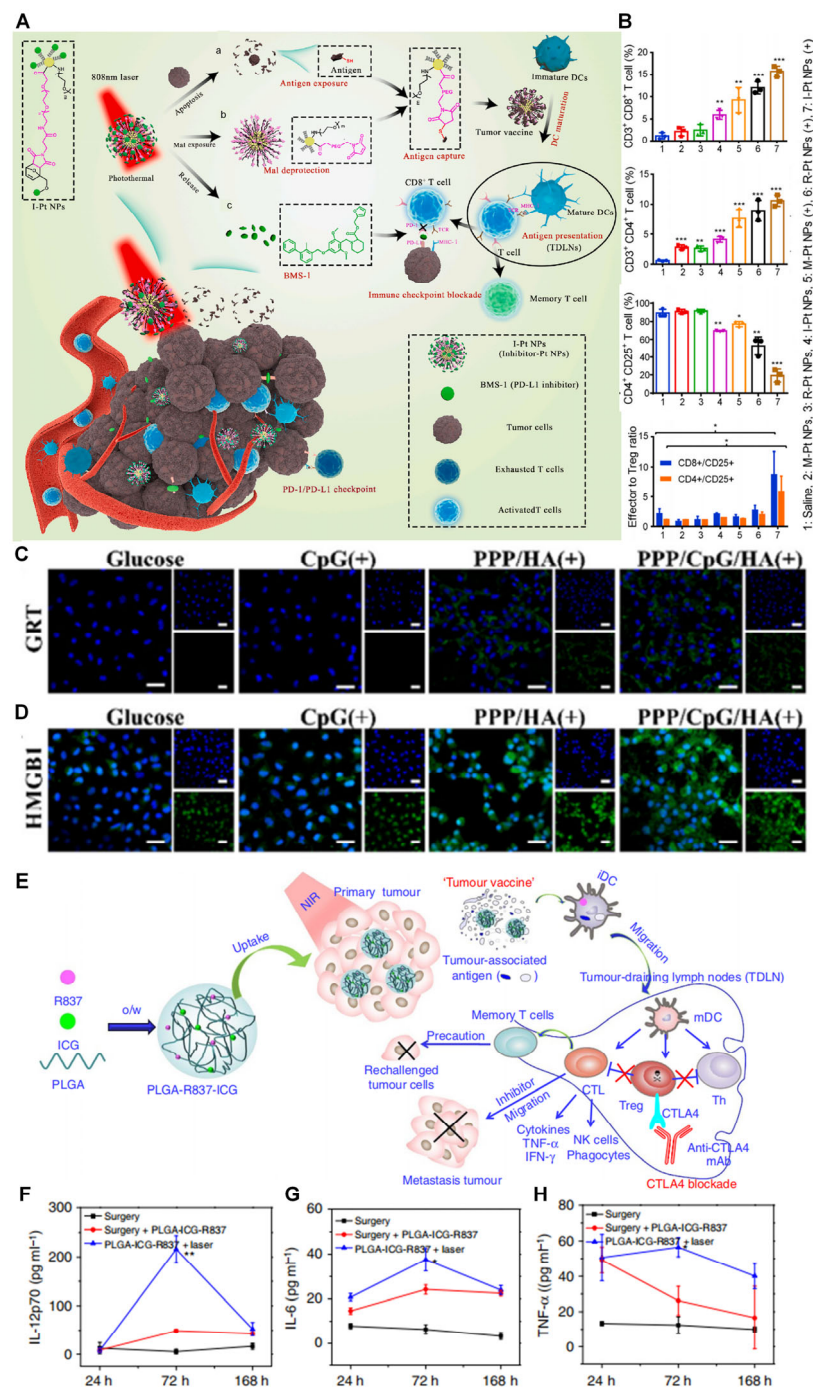


**Figure 5.** Example of nanomedicine-based cryoablation to activate immune responses. (**A**) Schematic illustration of the assembly of chitosan–TPP nanoparticles carrying trehalose and cryopreservation of

NK cells. (**B**) Schematic illustration of cryoablation-induced anti-tumor immunity. (**C**) Quantitation of CD56$^+$ NK cells in nanoparticle-treated and DMSO control NK cells by flow cytometry after cryoablation. (**D**–**F**) Nanoparticle-treated and DMSO control NK cells were challenged with K562 myelogenous leukemia cells at E: T ratios of 1:1, 5:1, and 10:1 for 4 h. Cytotoxicity against K562 cells (**D**), IFN-$\gamma$ production (**E**), and cell degranulation evaluated by CD107a expression (**F**) are shown (* $p < 0.05$).

## 2.6. Photothermal Ablation

Photothermal ablation (PTA) employs photothermal conversion agents to convert benign electromagnetic radiation, preferably near infrared (NIR) light, into heat to ablate cancer cells. The challenges PTA encounters include the limited penetration depth of the commonly used NIR-I laser (750–1000 nm), which makes PTA ineffective for deep-seated tumors, and the limited efficacy of PTA as a standalone therapy. Similar to other ablation therapy, PTA triggers the in situ release of TAAs and damage-associated molecular patterns (DAMPs) to elicit immune responses [86]. However, the immunosuppressive TME counteracts PTA-induced anti-tumor immunity. To overcome this problem, several therapeutic methods are used to boost PTA [87]. In this review, we focus on nanoparticles as drug carriers or immune adjuvants that work in synergy with PTA to achieve satisfactory therapeutic results. Yu and colleagues constructed polyethylene glycol-stabilized platinum nanoparticles conjugated with a PD-L1 inhibitor (BMS-1) via a thermo-sensitive linker. Upon exposure to NIR radiation, BMS-1 was released, and the nanoparticles captured TAAs from the ablated tumor cells, enhancing their internalization and presentation [56]. The nanoparticles also acted as immune adjuvants to enhance DC maturation. In addition, BMS-1 attenuated T cell depletion and promoted the infiltration of effector T cells into tumor tissues (Figure 6A,B). The microenvironment of solid tumors is usually characterized by hypoxia and weak acidity from lactic acid accumulation caused by hypoxia-driven metabolic reprogramming. Since lactic acid in the TME promotes tumor cell immune evasion by suppressing immune cell activity, increasing the metabolism of lactic acid is considered a plausible strategy for improving oncotherapy outcome. To this end, Zheng and colleagues constructed LOX-loaded, Cu$^{2+}$-chelated, PEG-modified mesoporous polydopamine (PDA) nanoparticles (mCULPs). Upon PTA exposure, mCULPs release LOX, which consumes lactate to $H_2O_2$. The resulting $H_2O_2$ is catalyzed by Cu$^{2+}$-chelated mesoporous PDA to produce oxygen, alleviating hypoxia in the TME and enhancing anti-tumor immunity [57]. Liang's study proposes a nanocomplex that delivers CDDP and PD-L1-targeted DNA aptamers to NSCLC tumors, releasing therapeutic cargos and Fe$^{2+}$ under the acidic tumor microenvironment. The nanocomplexes generate hydroxyl radicals to enhance chemotherapeutic efficacy and reverse immunologically "cold" tumors to "hot" tumors, providing a potential treatment paradigm for NSCLC [88]. Li and colleagues synthesized a PDA-based core–shell nanoplatform loaded with CpG ODN immunostimulants to trigger powerful PTA and anti-tumor immune response [58]. The cationized PDA core coated with a hyaluronic acid shell acted as an effective photothermal agent that increased tumor surface temperature by 16 °C and induced ICD (Figure 6C). Chen and colleagues synthesized PLGA-based nanoparticles composed of R837 and the photothermal agent ICG [59]. In NIR-induced laser ablation of primary tumors, the PLGA-ICG-R837 nanoparticles induced a strong immune response (Figure 6E–G). The PLGA-ICG-R837-enhanced PTA in combination with anti-CTLA4 checkpoint blockade immunotherapy suppressed regulatory T cells (Tregs) and inhibited metastasis and tumor recurrence in mice (Figure 6D).

**Figure 6.** Example of nanomedicine-based PTA to activate immune responses. (**A**) Schematic illustration of how BMS-1-conjugated Pt NPs boost PTA-induced anti-tumor immunity. (**B**) Effects of Pt NPs-assisted PTA on effector and regulatory T cells in secondary tumors. (**C**) Evaluation of ICD level by detection of calreticulin (CRT) and HMGB1 with confocal laser fluorescence microscopy. The scale bar represents 100 μm. "+" represents laser-treated. (**D**) Schematic illustration of anti-tumor immunity induced by PLGA-ICG-R837-assisted PTA in combination with checkpoint-blockade. (**E–H**) Cytokine levels in sera from mice isolated at specific time post different treatments (surgery, surgery and s.c. injection of PLGA-ICG-R837, i.t. injection of PLGA-ICG-R837 and PTA) (* $p < 0.05$, ** $p < 0.01$, *** $p < 0.001$).

## 2.7. Others

In recent years, several new ablation techniques have emerged in oncotherapy. These new methods, which include NanoKnife, terahertz (THz), electrodynamic, and NIR abla-

tion, can also be boosted by nanomaterials carrying chemotherapy or immunomodulatory agents. The NanoKnife procedure, which is based on irreversible electroporation (IRE), destroys tumor cells by releasing short pulses of high electric field. These pulses of high electric field create numerous irreversible nanoscale perforations on the tumor cell membrane, allowing molecules of different sizes to enter and exit cells freely, causing rapid apoptosis [89]. As NanoKnife is predominantly a nonthermal ablation technique, it can avoid the heat sink effect and prevent thermal injuries of non-targeted tissues such as blood vessels [90,91]. Recent studies have shown that IRE leads to the in situ release of large amounts of TAAs, which can act as tumor vaccines to induce anti-tumor immune response after ablation to kill the remaining tumor cells and inhibit local recurrence and distant metastasis. When used in combination with immunotherapy, NanoKnife can achieve synergistic effects against malignant tumors, with a broad application prospect in oncotherapy [92]. THz radiation (also referred to as THz waves) with frequencies ranging from 0.1 to 10 THz is widely used in military and security, as well as in medical imaging, diagnosis, and treatment. As an emerging new tool in medical diagnosis and treatment, THz radiation has considerable advantages over other more conventional radiation techniques. Firstly, unlike X-rays, THz radiation does not ionize biomolecules, so it does not damage human keratinocytes [93]. Secondly, the vibration, rotation, and oscillation of biomolecules and hydrogen bonds (which are abundant in water-based biological samples) are well spaced at THz frequency [94]. Thirdly, due to its much longer wavelength than that of visible light or infrared radiation, THz radiation propagates through biological tissues with much less scattering loss. The molecular spectra of molecules involved in cell metabolism (e.g., NO, CO, $O_2$, $CO_2$, and $\bullet$OH) are within the THz frequency range [95]. THz radiation is strongly absorbed by polar molecules such as water. The higher water content of cancer cells than normal cells make THz radiation a suitable method not only for detecting cancer cells, but also for destroying them. As such, THz radiation has been used to shrink tumors, and strong THz radiation has been used to treat skin cancer [96,97]. In electrochemical therapy, multiple electrodes are directly inserted into the tumor, and a direct current is applied to drastically change the pH value near the inserted electrodes, killing the surrounding cancer cells. The limited effective area of electrochemical therapy hinders its clinical application. To overcome this problem, platinum nanoparticles are introduced to catalyze the production of toxic reactive oxygen species (ROS) under oscillating electric field, in a procedure called electrodynamic therapy. Electrodynamic therapy exhibited an enhanced anti-tumor efficacy in a variety of cancers [98–101]. As a standalone therapy, electrodynamic therapy can effectively ablate tumors in ten minutes. However, achieving long-term tumor inhibition remains a great challenge, and single-session therapy can even increase the risk of tumor recurrence after treatment [102–104]. The combination of electrodynamic therapy and immunotherapy can reduce the recurrence rate to some extent. For instance, Chen and colleagues incorporated a chloride ion transporter (CIT) into fine Pt/Cu alloy nanoparticles ($PtCu_3$ NPs) for enhanced electrodynamic therapy [105]. CIT can increase intracellular $Cl^-$ concentration by transporting extracellular $Cl^-$. With the help of CIT, these modified nanoparticles can transform endogenous $H_2O_2$ into highly cytotoxic $\bullet$OH, deplete glutathione, and produce ROS effectively under an electric field. Electrodynamic therapy in combination with these nanoparticles achieved excellent anti-tumor efficacy in vitro and in vivo for relatively large tumors with a volume of approximately 500 $mm^3$. Chen's research team also incorporated 6-diazo-5-oxo-l-norleucine (DON), a glutamine antagonist, into Pt-Pd nanoparticles [60]. DON can prevent the production of glutathione, leading to decreased ROS clearance and increased ROS accumulation during electrodynamic therapy. DON synergized with electrodynamic therapy to induce DC maturation, $CD8^+$ T cell infiltration, and ICD, as well as the combined therapy demonstrated great efficacy inhibiting tumor growth, metastasis, and recurrence in animal models. Finally, NIR light can also be combined with nanomaterials for tumor ablation. Hirsch and colleagues first reported thermal therapy using a class of nanoparticles called metal nano-shells [106]. The metal nano-shells are composed of a spherical dielectric core of silica and a thin shell of

gold and have tunable optical resonances [107,108]. By tuning the nano-shells to strongly absorb NIR light, the nano-shells can be used to transform extracorporeally applied NIR light into heat energy for tumor ablation. In in vivo studies, exposure to NIR light in subcutaneous tumors injected with metal nano-shells raised tumor temperature by 37.4 °C and caused irreversible thermal damage in tumor cells [106].

### 3. Conclusions and Prospects

Compared with conventional surgical approaches in oncotherapy, tumor ablation techniques have the advantages of reduced invasiveness and pain, reduced adverse effects, faster recovery, simpler procedure, and greater cost-efficiency. However, ablation as a standalone therapy often suffers insufficient efficacy for larger tumors and high recurrence rate. Nanoplatform-based immunotherapy can work synergistically with ablation and amplify ablation-induced anti-tumor immunity. When used together in clinical practice, the appropriate combination therapy has the potential to eradicate primary tumors and prevent tumor metastasis and recurrence.

**Author Contributions:** Z.W. and X.Y. contributed equally to this work. Z.W. and X.Y. wrote the manuscript, M.H. and L.W. conceptualized and developed the idea, L.W. and C.L. revised manuscript and supervised this work. All authors have read and agreed to the published version of the manuscript.

**Institutional Review Board Statement:** Not applicable.

**Informed Consent Statement:** Not applicable.

**Data Availability Statement:** Not applicable.

**Conflicts of Interest:** The authors declare no conflict of interest.

### References

1. Dupuy, D.E. Tumor ablation: Treatment and palliation using image-guided therapy. *Oncology* **2005**, *19*, 4–5. [PubMed]
2. Goldberg, S.N.; Grassi, C.J.; Cardella, J.F.; Charboneau, J.W.; Gerald, D.; Dodd, I.; Dupuy, D.E.; Gervais, D.; Gillams, A.R.; Kane, R.A.; et al. Image-guided Tumor Ablation: Standardization of Terminology and Reporting Criteria. *Radiology* **2005**, *235*, 728–739. [CrossRef] [PubMed]
3. Bagchee-Clark, A.; Hwang, A.; Milovanovic, L. Image-Guided Tumor Ablative Therapies. In *Demystifying Interventional Radiology: A Guide for Medical Students*; Athreya, S., Albahhar, M., Eds.; Springer International Publishing: Cham, Switzerland, 2022; pp. 75–94. [CrossRef]
4. Zhu, H.; Cheng, P.; Chen, P.; Pu, K. Recent progress in the development of near-infrared organic photothermal and photodynamic nanotherapeutics. *Biomater. Sci.* **2018**, *6*, 746–765. [CrossRef] [PubMed]
5. Sugiura, N.; Takara, K.; Ohto, M.; Okuda, K.; Hirooka, N. Treatment of small hepatocellular carcinoma by percutaneous injection of ethanol into tumor with real-time ultrasound monitoring. *Acta Hepatol. Jpn.* **1983**, *24*, 920.
6. Livraghi, T.; Bajetta, E.; Matricardi, L.; Villa, E.; Lovati, R.; Vettori, C. Fine Needle Percutaneous Intratumoral Chemotherapy under Ultrasound Guidance: A Feasibility Study. *Tumori J.* **1986**, *72*, 81–87. [CrossRef]
7. Celikoglu, F.; Celikoglu, S.I.; Goldberg, E.P. Bronchoscopic intratumoral chemotherapy of lung cancer. *Lung Cancer* **2008**, *61*, 1–12. [CrossRef]
8. Livraghi, T.; Festi, D.; Monti, F.; Salmi, A.; Vettori, C. US-guided percutaneous alcohol injection of small hepatic and abdominal tumors. *Radiology* **1986**, *161*, 309–312. [CrossRef]
9. Livraghi, T.; Vettori, C. Percutaneous ethanol injection therapy of hepatoma. *Cardiovasc. Interv. Radiol.* **1990**, *13*, 146–152. [CrossRef]
10. Schoengen, A.; Binder, T.; Schiffelholz, W.; Schulz, P.C.; Zeelen, U. Fine-Needle Aspiration Guided by Ultrasound in Suspected Cancer. *Oncol. Res. Treat.* **1994**, *17*, 420–426. [CrossRef]
11. Livraghi, T.; Grigiori, W.; Mazziotti, A.; Sangalli, G.; Vettori, C. Percutaneous Alcohol Injection of Portal Thrombosis in Hepatocellular Carcinoma: A New Possible Treatment. *Tumori J.* **1990**, *76*, 394–397. [CrossRef]

12. Rossi, S.; Di Stasi, M.; Buscarini, E.; Cavanna, L.; Quaretti, P.; Squassante, E.; Garbagnati, F.; Buscarini, L. Percutaneous radiofrequency interstitial thermal ablation in the treatment of small hepatocellular carcinoma. *Cancer J. Sci. Am.* **1995**, *1*, 73–81.

13. Seki, T.; Wakabayashi, M.; Nakagawa, T.; Itho, T.; Shiro, T.; Kunieda, K.; Sato, M.; Uchiyama, S.; Inoue, K. Ultrasonically guided percutaneous microwave coagulation therapy for small hepatocellular carcinoma. *Cancer* **1994**, *74*, 817–825. [CrossRef]

14. Caracalos, A.; Levita, E.; Cooper, I.S. A study of roentgeno-anatomic lesion location and results in cryosurgery of the basal ganglia. *St. Barnabas Hosp. Med. Bull.* **1962**, *1*, 24–32. [PubMed]

15. Benninger, M.S.; Derakhshan, A.; Milstein, C.F. The Use of Cryotherapy for Papilloma and Early Laryngeal Cancers:Long-term Results. *Ann. Otol. Rhinol. Laryngol.* **2015**, *124*, 509–514. [CrossRef]

16. Waltz, J.M.; Aristizabal, G.; Riklan, M.; Cooper, I.S. Results of cryothalamectomy for parkinsonism in patients over 70. *J. Am. Geriatr. Soc.* **1967**, *15*, 1–8. [CrossRef]

17. Bahn, D.K.; Lee, F.; Badalament, R.; Kumar, A.; Greski, J.; Chernick, M. Targeted cryoablation of the prostate: 7-Year outcomes in the primary treatment of prostate cancer. *Urology* **2002**, *60*, 3–11. [CrossRef]

18. Waitz, R.; Solomon, S.B.; Petre, E.N.; Trumble, A.E.; Fassò, M.; Norton, L.; Allison, J.P. Potent Induction of Tumor Immunity by Combining Tumor Cryoablation with Anti-CTLA-4 Therapy. *Cancer Res.* **2012**, *72*, 430–439. [CrossRef]

19. Babaian, R.J.; Donnelly, B.; Bahn, D.; Baust, J.G.; Dineen, M.; Ellis, D.; Katz, A.; Pisters, L.; Rukstalis, D.; Shinohara, K.; et al. Best Practice Statement on Cryosurgery for the Treatment of Localized Prostate Cancer. *J. Urol.* **2008**, *180*, 1993–2004. [CrossRef]

20. Donnelly, B.J.; Saliken, J.C.; Brasher, P.M.A.; Ernst, S.D.; Rewcastle, J.C.; Lau, H.; Robinson, J.; Trpkov, K. A randomized trial of external beam radiotherapy versus cryoablation in patients with localized prostate cancer. *Cancer* **2010**, *116*, 323–330. [CrossRef]

21. Onik, G.; Vaughan, D.; Lotenfoe, R.; Dineen, M.; Brady, J. The "male lumpectomy": Focal therapy for prostate cancer using cryoablation results in 48 patients with at least 2-year follow-up. *Urol. Oncol. Semin. Orig. Investig.* **2008**, *26*, 500–505. [CrossRef]

22. Yu, Z.; Wang, D.; Qi, Y.; Zhou, T.; Rao, W.; Liu, J.; Hu, K. Autologous Cancer Cryoablation Mediated Nanovaccine Augments Systematic Immunotherapy. *Mater. Horiz.* **2023**. [CrossRef] [PubMed]

23. Ahmed, M.; Brace, C.L.; Fred, T.; Lee, J.; Goldberg, S.N. Principles of and Advances in Percutaneous Ablation. *Radiology* **2011**, *258*, 351–369. [CrossRef] [PubMed]

24. Puijk, R.S.; Ahmed, M.; Adam, A.; Arai, Y.; Arellano, R.; Baère, T.d.; Bale, R.; Bellera, C.; Binkert, C.A.; Brace, C.L.; et al. Consensus Guidelines for the Definition of Time-to-Event End Points in Image-guided Tumor Ablation: Results of the SIO and DATECAN Initiative. *Radiology* **2021**, *301*, 533–540. [CrossRef] [PubMed]

25. Ban, Q.; Bai, T.; Duan, X.; Kong, J. Noninvasive photothermal cancer therapy nanoplatforms via integrating nanomaterials and functional polymers. *Biomater. Sci.* **2017**, *5*, 190–210. [CrossRef]

26. Shang, T.; Yu, X.; Han, S.; Yang, B. Nanomedicine-based tumor photothermal therapy synergized immunotherapy. *Biomater. Sci.* **2020**, *8*, 5241–5259. [CrossRef]

27. Kok, H.P.; Cressman, E.N.K.; Ceelen, W.; Brace, C.L.; Ivkov, R.; Grüll, H.; ter Haar, G.; Wust, P.; Crezee, J. Heating technology for malignant tumors: A review. *Int. J. Hyperth.* **2020**, *37*, 711–741. [CrossRef]

28. Grasso, A.; Watkinson, A.F.; Tibballs, J.M.; Burroughs, A.K. Radiofrequency ablation in the treatment of hepatocellular carcinoma— A clinical viewpoint. *J. Hepatol.* **2000**, *33*, 667–672. [CrossRef]

29. Wang, K.; Wang, C.; Jiang, H.; Zhang, Y.; Lin, W.; Mo, J.; Jin, C. Combination of Ablation and Immunotherapy for Hepatocellular Carcinoma: Where We Are and Where to Go. *Front. Immunol.* **2021**, *12*, 792781. [CrossRef]

30. Li, X.; Liang, P. Immunotherapy for hepatocellular carcinoma following thermal ablation. *JBUON* **2014**, *19*, 867–871.

31. Naya, Y.; Nakamura, T.; Oishi, M.; Ueda, T.; Nakanishi, H.; Naitoh, Y.; Hongo, F.; Kamoi, K.; Okihara, K.; Tanaka, O.; et al. The efficacy of radio-frequency ablation for metastatic lung or liver tumors of male germ cell tumors as an alternative minimally invasive therapy after salvage chemotherapy. *Int. J. Clin. Oncol.* **2015**, *20*, 1192–1197. [CrossRef]

32. Camacho, J.C.; Petre, E.N.; Sofocleous, C.T. Thermal Ablation of Metastatic Colon Cancer to the Liver. *Semin. Interv. Radiol.* **2019**, *36*, 310–318. [CrossRef]

33. Kelekis, A.; Cornelis, F.H.; Tutton, S.; Filippiadis, D. Metastatic Osseous Pain Control: Bone Ablation and Cementoplasty. *Semin. Interv. Radiol* **2017**, *34*, 328–336. [CrossRef]

34. Lomas, D.J.; Woodrum, D.A.; Mynderse, L.A. Salvage ablation for locally recurrent prostate cancer. *Curr. Opin. Urol.* **2021**, *31*, 188–193. [CrossRef]

35. Agostinis, P.; Berg, K.; Cengel, K.A.; Foster, T.H.; Girotti, A.W.; Gollnick, S.O.; Hahn, S.M.; Hamblin, M.R.; Juzeniene, A.; Kessel, D.; et al. Photodynamic therapy of cancer: An update. *CA Cancer J. Clin.* **2011**, *61*, 250–281. [CrossRef]

36. Lerner, E.C.; Edwards, R.M.; Wilkinson, D.S.; Fecci, P.E. Laser ablation: Heating up the anti-tumor response in the intracranial compartment. *Adv. Drug Deliv. Rev.* **2022**, *185*, 114311. [CrossRef]

37. Xu, X.; Chen, Y.; Zhang, R.; Miao, X.; Chen, X. Activation of Anti-tumor Immune Response by Ablation of HCC with Nanosecond Pulsed Electric Field. *J. Clin. Transl. Hepatol.* **2018**, *6*, 85–88. [CrossRef]

38. Wu, F. Heat-Based Tumor Ablation: Role of the Immune Response. In *Therapeutic Ultrasound*; Escoffre, J.-M., Bouakaz, A., Eds.; Springer International Publishing: Cham, Switzerland, 2016; pp. 131–153. [CrossRef]

39. van den Bijgaart, R.J.E.; Schuurmans, F.; Fütterer, J.J.; Verheij, M.; Cornelissen, L.A.M.; Adema, G.J. Immune Modulation Plus Tumor Ablation: Adjuvants and Antibodies to Prime and Boost Anti-Tumor Immunity In Situ. *Front. Immunol.* **2021**, *12*, 617365. [CrossRef]

40. Qian, L.; Shen, Y.; Xie, J.; Meng, Z. Immunomodulatory effects of ablation therapy on tumors: Potentials for combination with immunotherapy. *Biochim. Biophys. Acta (BBA) Rev. Cancer* **2020**, *1874*, 188385. [CrossRef]

41. Ao, M.; Yu, F.; Li, Y.; Zhong, M.; Tang, Y.; Yang, H.; Wu, X.; Zhuang, Y.; Wang, H.; Sun, X.; et al. Carrier-free nanoparticles of camptothecin prodrug for chemo-photothermal therapy: The making, in vitro and in vivo testing. *J. Nanobiotechnol.* **2021**, *19*, 350. [CrossRef]

42. Wen, L.; Liu, H.; Hu, C.; Wei, Z.; Meng, Y.; Lu, C.; Su, Y.; Lu, L.; Liang, H.; Xu, Q. Thermoacoustic Imaging-Guided Thermo-Chemotherapy for Hepatocellular Carcinoma Sensitized by a Microwave-Responsive Nitric Oxide Nanogenerator. *ACS Appl. Mater. Interfaces* **2023**, *15*, 10477–10491. [CrossRef]

43. Ni, W.; Li, Y.; Liang, L.; Yang, S.; Zhan, M.; Lu, C.; Lu, L.; Wen, L. Tumor Microenvironment-Responsive Nanodrug for Clear-Cell Renal Cell Carcinoma Therapy via Triggering Waterfall-Like Cascade Ferroptosis. *J. Biomed. Nanotechnol.* **2022**, *18*, 327–342. [CrossRef] [PubMed]

44. Chen, J.; Chen, T.; Fang, Q.; Pan, C.; Akakuru, O.U.; Ren, W.; Lin, J.; Sheng, A.; Ma, X.; Wu, A. $Gd_2O_3$/b-$TiO_2$ composite nanoprobes with ultra-high photoconversion efficiency for MR image-guided NIR-II photothermal therapy. *Exploration* **2022**, *2*, 20220014. [CrossRef]

45. Doughty, A.C.V.; Hoover, A.R.; Layton, E.; Murray, C.K.; Howard, E.W.; Chen, W.R. Nanomaterial Applications in Photothermal Therapy for Cancer. *Materials* **2019**, *12*, 779. [CrossRef] [PubMed]

46. Jabir, N.R.; Tabrez, S.; Ashraf, G.M.; Shakil, S.; Damanhouri, G.A.; Kamal, M.A. Nanotechnology-based approaches in anticancer research. *Int. J. Nanomed.* **2012**, *7*, 4391–4408. [CrossRef]

47. Dai, H.; Fan, Q.; Wang, C. Recent applications of immunomodulatory biomaterials for disease immunotherapy. *Exploration* **2022**, *2*, 20210157. [CrossRef]

48. Yang, Z.; Zhu, Y.; Dong, Z.; Li, W.; Yang, N.; Wang, X.; Feng, L.; Liu, Z. Tumor-killing nanoreactors fueled by tumor debris can enhance radiofrequency ablation therapy and boost antitumor immune responses. *Nat. Commun.* **2021**, *12*, 4299. [CrossRef]

49. Li, L.; Zhang, H.; Zhao, H.; Shi, D.; Zheng, C.; Zhao, Y.; Yang, X. Radiofrequency-thermal effect of cisplatin-crosslinked nanogels for triple therapies of ablation-chemo-embolization. *Chem. Eng. J.* **2022**, *450*, 138421. [CrossRef]

50. Kuai, X.; Zhu, Y.; Yuan, Z.; Wang, S.; Lin, L.; Ye, X.; Lu, Y.; Luo, Y.; Pang, Z.; Geng, D.; et al. Perfluorooctyl bromide nanoemulsions holding $MnO_2$ nanoparticles with dual-modality imaging and glutathione depletion enhanced HIFU-eliciting tumor immunogenic cell death. *Acta Pharm. Sin. B* **2022**, *12*, 967–981. [CrossRef]

51. Han, X.; Wang, R.; Xu, J.; Chen, Q.; Liang, C.; Chen, J.; Zhao, J.; Chu, J.; Fan, Q.; Archibong, E.; et al. In situ thermal ablation of tumors in combination with nano-adjuvant and immune checkpoint blockade to inhibit cancer metastasis and recurrence. *Biomaterials* **2019**, *224*, 119490. [CrossRef]

52. Zhou, Q.; Gong, N.; Zhang, D.; Li, J.; Han, X.; Dou, J.; Huang, J.; Zhu, K.; Liang, P.; Liang, X.J.; et al. Mannose-Derived Carbon Dots Amplify Microwave Ablation-Induced Antitumor Immune Responses by Capturing and Transferring "Danger Signals" to Dendritic Cells. *ACS Nano* **2021**, *15*, 2920–2932. [CrossRef]

53. Li, S.Y.; Zhu, C.Y.; Zhou, X.L.; Chen, L.; Bo, X.W.; Shen, Y.T.; Guan, X.; Han, X.X.; Shan, D.D.; Sun, L.P.; et al. Engineering ROS-Responsive Bioscaffolds for Disrupting Myeloid Cell-Driven Immunosuppressive Niche to Enhance PD-L1 Blockade-Based Postablative Immunotherapy. *Adv. Sci.* **2022**, *9*, 2104619. [CrossRef]

54. Pan, J.; Hu, P.; Guo, Y.; Hao, J.; Ni, D.; Xu, Y.; Bao, Q.; Yao, H.; Wei, C.; Wu, Q.; et al. Combined Magnetic Hyperthermia and Immune Therapy for Primary and Metastatic Tumor Treatments. *ACS Nano* **2020**, *14*, 1033–1044. [CrossRef]

55. Liu, X.; Yan, B.; Li, Y.; Ma, X.; Jiao, W.; Shi, K.; Zhang, T.; Chen, S.; He, Y.; Liang, X.-J.; et al. Graphene Oxide-Grafted Magnetic Nanorings Mediated Magnetothermodynamic Therapy Favoring Reactive Oxygen Species-Related Immune Response for Enhanced Antitumor Efficacy. *ACS Nano* **2020**, *14*, 1936–1950. [CrossRef]

56. Yu, J.; Liu, S.; Wang, Y.P.; He, X.D.; Zhang, Q.F.; Qi, Y.X.; Zhou, D.F.; Xie, Z.G.; Li, X.Y.; Huang, Y.B. Synergistic enhancement of immunological responses triggered by hyperthermia sensitive Pt NPs via NIR laser to inhibit cancer relapse and metastasis. *Bioact. Mater.* **2022**, *7*, 389–400. [CrossRef]

57. Zheng, X.; Liu, Y.; Liu, Y.; Zhang, T.; Zhao, Y.; Zang, J.; Yang, Y.; He, R.; Chong, G.; Ruan, S.; et al. Dual Closed-Loop of Catalyzed Lactate Depletion and Immune Response to Potentiate Photothermal Immunotherapy. *ACS Appl. Mater. Interfaces* **2022**, *14*, 23260–23276. [CrossRef]

58. Li, M.; Guo, R.; Wei, J.; Deng, M.; Li, J.; Tao, Y.; Li, M.; He, Q. Polydopamine-based nanoplatform for photothermal ablation with long-term immune activation against melanoma and its recurrence. *Acta Biomater.* **2021**, *136*, 546–557. [CrossRef]

59. Chen, Q.; Xu, L.; Liang, C.; Wang, C.; Peng, R.; Liu, Z. Photothermal therapy with immune-adjuvant nanoparticles together with checkpoint blockade for effective cancer immunotherapy. *Nat. Commun.* **2016**, *7*, 13193. [CrossRef]

60. Chen, G.; Xu, Q.; Feng, Z.; Xu, Q.; Zhang, X.; Yang, Y.; Zhang, Y.; Liang, X.J.; Yu, Z.; Yu, M. Glutamine Antagonist Synergizes with Electrodynamic Therapy to Induce Tumor Regression and Systemic Antitumor Immunity. *ACS Nano* **2022**, *16*, 951–962. [CrossRef]

61. European Association for the Study of the Liver. EASL Clinical Practice Guidelines: Management of hepatocellular carcinoma. *J. Hepatol.* **2018**, *69*, 182–236. [CrossRef]

62. Cucchetti, A.; Piscaglia, F.; Cescon, M.; Colecchia, A.; Ercolani, G.; Bolondi, L.; Pinna, A.D. Cost-effectiveness of hepatic resection versus percutaneous radiofrequency ablation for early hepatocellular carcinoma. *J. Hepatol.* **2013**, *59*, 300–307. [CrossRef]

63. Liu, Q.; Zhai, B.; Yang, W.; Yu, L.-X.; Dong, W.; He, Y.-Q.; Chen, L.; Tang, L.; Lin, Y.; Huang, D.-D.; et al. Abrogation of Local Cancer Recurrence After Radiofrequency Ablation by Dendritic Cell-Based Hyperthermic Tumor Vaccine. *Mol. Ther.* **2009**, *17*, 2049–2057. [CrossRef]

64. Cao, Y.; Zhu, X.; Hossen, M.N.; Kakar, P.; Zhao, Y.; Chen, X. Augmentation of vaccine-induced humoral and cellular immunity by a physical radiofrequency adjuvant. *Nat. Commun.* **2018**, *9*, 3695. [CrossRef] [PubMed]

65. Mai, X.; Chang, Y.; You, Y.; He, L.; Chen, T. Designing intelligent nano-bomb with on-demand site-specific drug burst release to synergize with high-intensity focused ultrasound cancer ablation. *J. Control. Release* **2021**, *331*, 270–281. [CrossRef] [PubMed]

66. Li, Y.; Patel, S.P.; Roszik, J.; Qin, Y. Hypoxia-Driven Immunosuppressive Metabolites in the Tumor Microenvironment: New Approaches for Combinational Immunotherapy. *Front. Immunol.* **2018**, *9*, 1591. [CrossRef] [PubMed]

67. Ma, X.; Yao, M.; Shi, J.; Li, X.; Gao, Y.; Luo, Q.; Hou, R.; Liang, X.; Wang, F. High Intensity Focused Ultrasound-Responsive and Ultrastable Cerasomal Perfluorocarbon Nanodroplets for Alleviating Tumor Multidrug Resistance and Epithelial-Mesenchymal Transition. *ACS Nano* **2020**, *14*, 15904–15918. [CrossRef] [PubMed]

68. Chu, K.F.; Dupuy, D.E. Thermal ablation of tumours: Biological mechanisms and advances in therapy. *Nat. Rev. Cancer* **2014**, *14*, 199–208. [CrossRef]

69. Zhu, Y.; Yang, Z.; Pan, Z.; Hao, Y.; Wang, C.; Dong, Z.; Li, Q.; Han, Y.; Tian, L.; Feng, L.; et al. Metallo-alginate hydrogel can potentiate microwave tumor ablation for synergistic cancer treatment. *Sci. Adv.* **2022**, *8*, eabo5285. [CrossRef]

70. Yan, Y.; Gong, J.; Chen, J.; Zeng, Z.; Huang, W.; Pu, K.; Liu, J.; Chen, P. Recent Advances on Graphene Quantum Dots: From Chemistry and Physics to Applications. *Adv. Mater.* **2019**, *31*, 1808283. [CrossRef]

71. Chao, Y.; Chen, Q.; Liu, Z. Smart Injectable Hydrogels for Cancer Immunotherapy. *Adv. Funct. Mater.* **2020**, *30*, 1902785. [CrossRef]

72. Gao, Y.; Zhou, Y.; Pan, J.; Zhong, X.; Ding, J.; Jing, X.; Sun, S. A general strategy towards an injectable microwave-sensitive immune hydrogel for combined percutaneous microwave ablation and immunotherapy. *Chem. Eng. J.* **2021**, *422*, 130111. [CrossRef]

73. Shen, Y.T.; Chen, L.; Guan, X.; Han, X.X.; Bo, X.W.; Li, S.Y.; Sun, L.P.; Chen, Y.; Yue, W.W.; Xu, H.X. Tailoring Chemoimmunostimulant Bioscaffolds for Inhibiting Tumor Growth and Metastasis after Incomplete Microwave Ablation. *Acs Nano* **2021**, *15*, 20414–20429. [CrossRef]

74. Yan, S.; Zhang, D.; Gu, N.; Zheng, J.; Ding, A.; Wang, Z.; Xing, B.; Ma, M.; Zhang, Y. Therapeutic effect of Fe2O3 nanoparticles combined with magnetic fluid hyperthermia on cultured liver cancer cells and xenograft liver cancers. *J. Nanosci. Nanotechnol.* **2005**, *5*, 1185–1192. [CrossRef]

75. Sadhukha, T.; Wiedmann, T.S.; Panyam, J. Inhalable magnetic nanoparticles for targeted hyperthermia in lung cancer therapy. *Biomaterials* **2013**, *34*, 5163–5171. [CrossRef]

76. Johannsen, M.; Gneveckow, U.; Eckelt, L.; Feussner, A.; Waldofner, N.; Scholz, R.; Deger, S.; Wust, P.; Loening, S.A.; Jordan, A. Clinical hyperthermia of prostate cancer using magnetic nanoparticles: Presentation of a new interstitial technique. *Int. J. Hyperth.* **2005**, *21*, 637–647. [CrossRef]

77. Thiesen, B.; Jordan, A. Clinical applications of magnetic nanoparticles for hyperthermia. *Int. J. Hyperth.* **2008**, *24*, 467–474. [CrossRef]

78. Olagunju, A.; Forsman, T.; Ward, R.C. An update on the use of cryoablation and immunotherapy for breast cancer. *Front. Immunol.* **2022**, *13*, 1026475. [CrossRef]

79. Yakkala, C.; Denys, A.; Kandalaft, L.; Duran, R. Cryoablation and immunotherapy of cancer. *Curr. Opin. Biotechnol.* **2020**, *65*, 60–64. [CrossRef]

80. He, X.Z.; Wang, Q.F.; Han, S.; Wang, H.Q.; Ye, Y.Y.; Zhu, Z.Y.; Zhang, S.Z. Cryo-ablation improves anti-tumor immunity through recovering tumor educated dendritic cells in tumor-draining lymph nodes. *Drug Des. Dev. Ther.* **2015**, *9*, 1449–1458. [CrossRef]

81. Izawa, J.I.; Madsen, L.T.; Scott, S.M.; Tran, J.P.; McGuire, E.J.; Von Eschenbach, A.C.; Pisters, L.L. Salvage cryotherapy for recurrent prostate cancer after radiotherapy: Variables affecting patient outcome. *J. Clin. Oncol.* **2002**, *20*, 2664–2671. [CrossRef]

82. Chodez, M.; Fiard, G.; Arnoux, V.; Descotes, J.L.; Long, J.A. Les traitements ablatifs dans le cancer du rein localisé: Revue de la littérature en 2014. *Prog. Urol.* **2015**, *25*, 499–509. [CrossRef]

83. Wang, H.; Agarwal, P.; Liang, Y.; Xu, J.; Zhao, G.; Tkaczuk, K.H.R.; Lu, X.; He, X. Enhanced cancer therapy with cold-controlled drug release and photothermal warming enabled by one nanoplatform. *Biomaterials* **2018**, *180*, 265–278. [CrossRef]

84. Yao, X.; Jovevski, J.J.; Todd, M.F.; Xu, R.; Li, Y.; Wang, J.; Matosevic, S. Nanoparticle-Mediated Intracellular Protection of Natural Killer Cells Avoids Cryoinjury and Retains Potent Antitumor Functions. *Adv. Sci.* **2020**, *7*, 1902938. [CrossRef]

85. Kwak, K.; Yu, B.; Lewandowski, R.J.; Kim, D.H. Recent progress in cryoablation cancer therapy and nanoparticles mediated cryoablation. *Theranostics* **2022**, *12*, 2175–2204. [CrossRef] [PubMed]

86. Ma, Y.; Xiao, F.; Lu, C.; Wen, L. Multifunctional Nanosystems Powered Photodynamic Immunotherapy. *Front. Pharmacol.* **2022**, *13*, 905078. [CrossRef] [PubMed]

87. Jiang, Z.; Li, T.; Cheng, H.; Zhang, F.; Yang, X.; Wang, S.; Zhou, J.; Ding, Y. Nanomedicine potentiates mild photothermal therapy for tumor ablation. *Asian J. Pharm. Sci.* **2021**, *16*, 738–761. [CrossRef] [PubMed]

88. Liang, L.; Wen, L.; Weng, Y.; Song, J.; Li, H.; Zhang, Y.; He, X.; Zhao, W.; Zhan, M.; Li, Y.; et al. Homologous-targeted and tumor microenvironment-activated hydroxyl radical nanogenerator for enhanced chemoimmunotherapy of non-small cell lung cancer. *Chem. Eng. J.* **2021**, *425*, 131451. [CrossRef]

89. Weiss, M.J.; Wolfgang, C.L. Irreversible electroporation: A novel therapy for stage III pancreatic cancer. *Adv. Surg.* **2014**, *48*, 253–258. [CrossRef]

90.  Narayanan, G.; Froud, T.; Suthar, R.; Barbery, K. Irreversible electroporation of hepatic malignancy. *Semin. Interv. Radiol.* **2013**, *30*, 67–73. [CrossRef]

91.  Chan, G.; Pua, U. Irreversible Electroporation of the Pancreas. *Semin. Interv. Radiol.* **2019**, *36*, 213–220. [CrossRef]

92.  Zhang, N.; Li, Z.; Han, X.; Zhu, Z.; Li, Z.; Zhao, Y.; Liu, Z.; Lv, Y. Irreversible Electroporation: An Emerging Immunomodulatory Therapy on Solid Tumors. *Front. Immunol.* **2022**, *12*, 811726. [CrossRef]

93.  Berry, E.; Walker, G.C.; Fitzgerald, A.J.; Zinov'ev, N.N.; Chamberlain, M.; Smye, S.W.; Miles, R.E.; Smith, M.A. Do in vivo terahertz imaging systems comply with safety guidelines. *J. Laser Appl.* **2003**, *15*, 192–198. [CrossRef]

94.  Amini, T.; Jahangiri, F.; Ameri, Z.; Hemmatian, M.A. A Review of Feasible Applications of THz Waves in Medical Diagnostics and Treatments. *J. Lasers Med. Sci.* **2021**, *12*, e92. [CrossRef]

95.  Parshina, S.S.; Kirichuk, V.F.; Tupikin, V.D.; Golovacheva, T.V.; Krenitskiy, A.P.; Majborodin, A.V. Terahertz therapy—A new method of treatment of cardiovascular pathology. In Proceedings of the 2005 Joint 30th International Conference on Infrared and Millimeter Waves and 13th International Conference on Terahertz Electronics, Williamsburg, VA, USA, 19–23 September 2005; Volume 311, pp. 311–312.

96.  Fedorov, V.I. The biological effects of terahertz laser radiation as a fundamental premise for designing diagnostic and treatment methods. *Biophysics* **2017**, *62*, 324–330. [CrossRef]

97.  Titova, L.V.; Ayesheshim, A.K.; Golubov, A.; Rodriguez-Juarez, R.; Woycicki, R.; Hegmann, F.A.; Kovalchuk, O. Intense THz pulses down-regulate genes associated with skin cancer and psoriasis: A new therapeutic avenue? *Sci. Rep.* **2013**, *3*, 2363. [CrossRef]

98.  Chen, T.; Gu, T.; Cheng, L.; Li, X.; Han, G.; Liu, Z. Porous Pt nanoparticles loaded with doxorubicin to enable synergistic Chemo-/Electrodynamic Therapy. *Biomaterials* **2020**, *255*, 120202. [CrossRef]

99.  Gu, T.; Wang, Y.; Lu, Y.; Cheng, L.; Feng, L.; Zhang, H.; Li, X.; Han, G.; Liu, Z. Platinum Nanoparticles to Enable Electrodynamic Therapy for Effective Cancer Treatment. *Adv. Mater.* **2019**, *31*, e1806803. [CrossRef]

100.  Gu, T.; Chen, T.; Cheng, L.; Li, X.; Han, G.; Liu, Z. Mesoporous silica decorated with platinum nanoparticles for drug delivery and synergistic electrodynamic chemotherapy. *Nano Res.* **2020**, *13*, 2209–2215. [CrossRef]

101.  Lu, Z.; Gao, J.; Fang, C.; Zhou, Y.; Li, X.; Han, G. Porous Pt Nanospheres Incorporated with GOx to Enable Synergistic Oxygen-Inductive Starvation/Electrodynamic Tumor Therapy. *Adv. Sci.* **2020**, *7*, 2001223. [CrossRef]

102.  Li, W.; Yang, J.; Luo, L.; Jiang, M.; Qin, B.; Yin, H.; Zhu, C.; Yuan, X.; Zhang, J.; Luo, Z.; et al. Targeting photodynamic and photothermal therapy to the endoplasmic reticulum enhances immunogenic cancer cell death. *Nat. Commun.* **2019**, *10*, 3349. [CrossRef]

103.  Chen, S.; Li, D.; Du, X. Carrier-Free Nanoassembly of Doxorubicin Prodrug and Sirna for Combinationally Inducing Immunogenic Cell Death and Reversing Immunosuppression. *Nano Today* **2020**, *35*, 100924. [CrossRef]

104.  Wang, H.; Wang, K.; He, L.; Liu, Y.; Dong, H.; Li, Y. Engineering antigen as photosensitiser nanocarrier to facilitate ROS triggered immune cascade for photodynamic immunotherapy. *Biomaterials* **2020**, *244*, 119964. [CrossRef] [PubMed]

105.  Chen, T.; Han, G.; Li, X. Platinum-copper alloy nanoparticles armored with chloride ion transporter to promote electro-driven tumor inhibition. *Bioact. Mater.* **2022**, *12*, 143–152. [CrossRef] [PubMed]

106.  Hirsch, L.R.; Stafford, R.J.; Bankson, J.A.; Sershen, S.R.; Rivera, B.; Price, R.E.; Hazle, J.D.; Halas, N.J.; West, J.L. Nanoshell-mediated near-infrared thermal therapy of tumors under magnetic resonance guidance. *Proc. Natl. Acad. Sci. USA* **2003**, *100*, 13549–13554. [CrossRef] [PubMed]

107.  Averitt, R.D.; Westcott, S.L.; Halas, N.J. Linear optical properties of gold nanoshells. *J. Opt. Soc. Am. B* **1999**, *16*, 1824–1832. [CrossRef]

108.  Oldenburg, S.J.; Averitt, R.D.; Westcott, S.L.; Halas, N.J. Nanoengineering of optical resonances. *Chem. Phys. Lett.* **1998**, *288*, 243–247. [CrossRef]